Etching with electron beam generated plasmas

D. Leonhardt,[a] S. G. Walton, C. Muratore,[b] R. F. Fernsler, and R. A. Meger
U.S. Naval Research Laboratory, Plasma Physics Division, Washington, D.C. 20375

(Received 6 February 2004; accepted 26 July 2004; published 7 October 2004)

A modulated electron beam generated plasma has been used to dry etch standard photoresist materials and silicon. Oxygen–argon mixtures were used to etch organic resist material and sulfur hexafluoride mixed with argon or oxygen was used for the silicon etching. Etch rates and anisotropy were determined with respect to gas compositions, incident ion energy (from an applied rf bias) and plasma duty factor. For 1818 negative resist and i-line resists the removal rate increased nearly linearly with ion energy (up to 220 nm/min at 100 eV), with reasonable anisotropic pattern transfer above 50 eV. Little change in etch rate was seen as gas composition went from pure oxygen to 70% argon, implying the resist removal mechanism in this system required the additional energy supplied by the ions. With silicon substrates at room temperature, mixtures of argon and sulfur hexafluoride etched approximately seven times faster (1375 nm/min) than mixtures of oxygen and sulfur hexafluoride (~200 nm/min) with 200 eV ions, the difference is attributed to the passivation of the silicon by involatile silicon oxyfluoride (SiO_xF_y) compounds. At low incident ion energies, the $Ar-SF_6$ mixtures showed a strong chemical (lateral) etch component before an ion-assisted regime, which started at ~75 eV. Etch rates were independent of the 0.5%–50% duty factors studied in this work. [DOI: 10.1116/1.1795827]

I. INTRODUCTION

Both silicon[1–3] and photoresist[4–7] material removal in high-density plasma sources have been discussed in scientific literature. The removal rates and mechanisms are well documented for a variety of gas compositions, although the dry etching of these materials is not completely understood, usually due to nuances between plasma sources and their respective gas-phase plasma chemistries. Furthermore, etching continues to evolve as more applications and environmentally safe gases are found. This is particularly true for micro-electro mechanical devices (MEMS) where deep, micron-sized features in silicon are desired. Deep etch techniques consume large amounts of reactive gas, and the low toxicity of sulfur hexafluoride has resulted in a resurgence in its popularity as an etching precursor. To control feature evolution, intermittent passivation steps are used to inhibit undercutting.[8] These passivation-etch multi-step processes inhibit the chemical (isotropic) etch component and allow processing to be done at room temperature rather than cryogenic temperatures. For applications containing polymer materials, substrates are typically sensitive to high-density plasma environments, showing undesirable effects such as melting or graphitization from heating and excessive ion bombardment. For widely used plasma cleaning (ashing) processes, where the goal is complete removal of organic material, the sensitivity is not an issue. However, if anisotropic pattern transfer is desired, many high-density plasma sources can induce excessive damage in delicate materials.

In this paper, some general chemistries associated with the etching of silicon and photoresist are applied to electron beam (e beam) generated plasmas. The Naval Research Laboratory has developed a Large Area Plasma Processing System (LAPPS) that uses a high-energy electron beam to initiate gas ionization. This system has been discussed previously both theoretically[9,10] and experimentally.[11,12] Generally, sheet electron beams are used to ionize background gas to produce planar high-density plasmas with very cold plasma electron energy distributions and low internal electric fields. Because the high-energy electron beam initiates gas ionization, nearly *all* electron-induced reactions are available and ionization is favored because its cross section is largest. Since the secondary (plasma) electron distribution is not driving the plasma production, plasma electrons are cooled by additional (elastic and inelastic) collisions with the background gas to energies commensurate to the lowest energy process available, which is typically vibrational excitations below 1 eV. The plasma electron temperature (and plasma potential) is thus significantly lower in an e beam produced plasma than in conventional plasma discharges, which are driven by electric fields that heat plasma electrons to reach the lowest gas ionization potential and sustain the discharge. The majority of the plasma electrons nevertheless have energies below the ionization threshold, so most of the discharge energy goes into inelastic excitation rather than ionization. This is an inefficient use of power since (1) only a small portion of the plasma electron distribution actually ionizes the gas and (2) the electrons are constantly heated from room temperature to maintain ionization, thereby constantly driving the low-energy reactions. Since dissociation mimics ionization (albeit at lower threshold energies), conventional discharges are similarly inefficient at gas dissociation, requiring higher energies (per reaction) than electron beam-driven processes.

The goal of this work was to determine the capabilities and limitations of this e beam generated plasma to produce

[a]Electronic mail: darrin@ccs.nrl.navy.mil
[b]ASEE/NRL Postdoctoral Research Associate.

reactive gas phase components and interact with substrates. The low electron temperatures and plasma fields allow better ion energy control and anisotropy, while the e beam ionization mechanism is capable of producing a wider range of ion flux from the gas constituents in the etching of various materials. In addition, due to the highly localized ionization source (the e beam) a greater variation in the ion and neutral flux is possible, by adjusting the distance between the substrate and e beam. In order to consider these plasma's unique qualities in etching applications, substrates of polymer-type materials and silicon were etched at room temperature in plasmas of various gas mixtures. For the polymer materials (photoresist), $Ar-O_2$ mixtures were used to determine a process for anisotropic material removal. Silicon substrates were similarly etched using SF_6-based mixtures at various ion energies and gas flows. The $Ar-SF_6$ mixtures were used as a baseline for typical plasma chemistries, while the O_2-SF_6 mixtures were studied to increase the viability of anisotropic room temperature silicon etching in this system through passivating oxide films. The O_2-rich plasmas showed significant surface passivation, while the $Ar-SF_6$ mixtures demonstrated a strong chemical etch at room temperature.

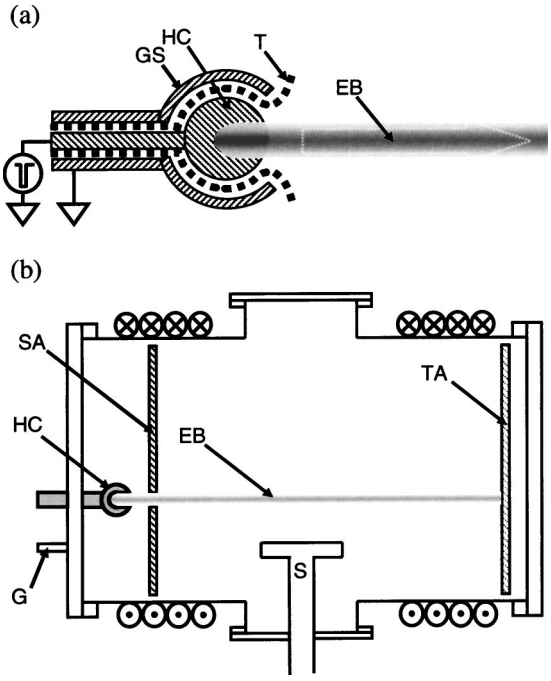

FIG. 1. Schematic diagram of the (a) hollow cathode e beam source and (b) etching system. Labeled components are: Ground shield (GS), hollow cathode (HC), Teflon® insulation (T), electron beam/plasma (EB), slotted anode (SA), termination anode (TA), gas feed (G), and etching stage (S). The Helmholtz coils are designated by crosses and dots on the outside of the chamber.

II. EXPERIMENT

A. Electron beam generation and plasma production

A linear hollow cathode operating in a uniform magnetic field was used to produce a high-energy electron beam. The hollow cathode was constructed from 28 cm length of brass bar stock (~2 cm diameter) with a 1 cm wide by 1.5 cm deep channel, 25 cm along the length and polished to a mirror-like finish. A Telfon® sheet insulated the hollow cathode from a surrounding ground shield, which provided structural support and a local ground for the high voltage signal. Figure 1(a) shows the cross sectional view of the cathode assembly.

The cathode was powered by −2 kV pulses, 0.5–10 ms in duration at various repetition rates to produce duty factors of 0.5%–50%. These pulses were provided by a homemade pulser unit[13] that provided the typical cathode operating current of ~50 mA/pulse. A grounded anode was located ≈6 cm in front of the cathode and was made from 3 mm thick stainless steel plate and shim stock. The shim stock provided a 25 cm × 1 cm slot to define the shape of the electron beam entering the processing region. A similar anode, without a slot, was located ≈50 cm away and was the termination for the e beam. These components were located in a cylindrical aluminum vacuum chamber with a 48 cm inner diameter. A base vacuum of $\sim 5 \times 10^{-7}$ Torr was provided by a 150 l/s turbomolecular pump, and gas flow was provided by mass flow controllers. Operating pressure was set by a fixed total gas flow for the mixture and the turbo pump was throttled to get the desired total operating pressure, measured by a capacitance manometer gauge (MKS). A set of Helmholtz coils (~3 Gauss/amp) were wound directly onto the chamber with magnet wire to reduce scattering of the e beam. A 165 Gauss magnetic field, uniform to +/−2% over the entire area of the e beam, collimated the emergent 2 keV e beam over the length of the chamber. For this work, the cathode and slot were positioned 7.5 cm off of the chamber center axis for convenience. The cathode, chamber and etching stage are shown in Fig. 1(b).

B. Etching arrangement

An etching stage was constructed from stainless steel, copper, and boron nitride materials. The front of the stage was a 13 cm diam stainless steel plate recessed flush into a 13.5 cm boron nitride disk (0.6 cm thick). The front electrode was electrically isolated from the stage body so that an rf bias could be applied to increase the incident energy of plasma ions. The body housed a water cooling line and a shielded K-type thermocouple was embedded into the boron nitride insulator, close to the front electrode.

Rf power was applied to the stage through a commercial matchbox (RFPP Model AM-5) by a rf amplifier/signal generator operating at 13.56 MHz. In order to minimize undesired rf discharges and to produce results well correlated to the e beam produced plasma, rf power was only applied during the e beam pulse, after a short (100–150 μs) delay to avoid any transient cathode ignition behavior. Matching or coupling of the applied rf voltage to the plasma was considered to be optimized when the rf-induced dc self-bias ("rf bias") and rf signal amplitude were at a maximum. Measurements of the rf voltage and currents to the stage were done in air at the electrical feedthrough with a 10× oscilloscope

probe and current transformer (Pearson Electronics Model 2877). These measurements showed that the stage reached steady-state bias values within 200 μs of the rf signal application. Additional measurements of forward and reflected rf power with an inline directional coupler (Bird Electronics) showed that >85% of the rf power was coupled to the plasma through the stage at these conditions. Etching times (τ_{etch}) correspond to the total time rf was applied to the sample, which was slightly less than the time the e beam produced plasma was on, due to the delay mentioned previously. Actual laboratory time would be the reported exposure time divided by the duty factor.

In all experiments, 0.5–1 cm^2 samples were cut from larger substrates and adhered to the stage with silver print epoxy. The stage temperature was kept at 20±4 °C during all experiments. Silicon wafers were used as substrates for the resist samples. Thick coatings (~3 microns) of negative-type photoresist (Shipley 1818) were masked with a chrome sample pattern of 5–100 μm features. The i-line resist samples were patterned with a copper mask containing 300 nm vias. These i-line samples were exposed to a standard semiconductor industry ashing process and rinsed with distilled water prior to these experiments. Etch depth (ED) was determined by scanning electron microscope (SEM) analysis at various locations on the sample and then was divided by the etch time (τ_{etch}) to calculate the etch rate ($ER = ED/\tau_{etch}$).

For the silicon etching, similarly sized samples were cut from patterned (SiO_2 mask thermally grown) and unpatterned silicon ⟨100⟩ wafers. The unpatterned silicon samples were partially masked with the silver print epoxy. Etch depths were measured on the unpatterned samples after the mask was removed with a Tencor (P-10) profilometer to calculate the etch rates as discussed above. All errors shown in etch rate are from multiple etch depth determinations on single samples. SEM analysis was used to look at selected feature evolution on the patterned samples.

"Standard" etching conditions were set by the cathode operating at a 10% duty factor with a 2.1 ms, −2 kV pulse in a 165 G magnetic field with the sample located 8 mm from the e beam edge. For resist etching, a 55 mTorr oxygen operating pressure (50 sccm) was used, which provided[11] a low temperature (≈0.5 eV), high-density plasma ($\approx 2 \times 10^{11}$ cm^{-3}). Similar operating conditions were used for silicon etching in 70 mTorr of $Ar-SF_6$ mixtures (35:15 by flow, respectively) and 60 mTorr of O_2-SF_6 mixtures (56:8 by flow). Similar plasma densities and temperatures were observed in these mixtures as well.

III. DATA AND RESULTS

A. Photoresist etching

The variation of the negative resist etch rate (ER) with respect to the incident ion energy is shown in Fig. 2. Because the plasma potential associated with these systems is low[11,12] (<5 V), the incident ion energy has been taken to be the measured rf bias[14] in all of these experiments. Etching time varied from 2 to 6 min, depending on the ion energy. A moderately linear relationship between ion energy and ER was seen, although at higher voltages the ER increase was somewhat greater. When ion energies were below 50 eV, significant undercutting at the mask–resist interface was seen in the patterned samples. Anisotropic feature profiles appeared when the ion energy was increased above 50 eV, although vertical profiles were not observed until the ion energy reached 100 eV in the larger features. While feature anisotropy increased with ion energy, the surface of the organic material was also roughened at high ion energies. Figure 3 shows the ashed via structure as received, then after 50 and 100 eV etches (top, middle, and bottom, respectively). The 50 eV etch was 3 min and the 100 eV etch was for 1.5 min. After the 50 eV etch, the fine spires left behind from the commercial ash process were removed. The 100 eV etch also removed the spires, but left residue around the via edge.

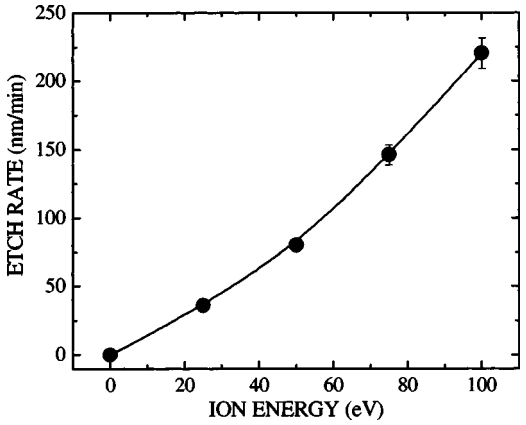

FIG. 2. Etch rate dependence of negative resist material on incident ion energy in a 55 mTorr O_2 plasma.

Figure 4 shows the negative resist relative ER as a function of the oxygen concentration in the process gas mixture. The etch rate remained fairly constant until the oxygen percentage dropped below 30%. It should be noted that in these experiments the total pressure of the mixtures was 65 mTorr, but was 55 mTorr for pure O_2 and 80 mTorr for pure Ar. In all cases the cathode operation was very similar, but the plasma density was slightly higher in the case of the mixtures and approximately twice as high in the pure Ar case. No effect in ER was seen as the duty cycle of the plasma was varied from 0.5% to 50% while keeping the total exposure time constant (i.e., only changing the relative duration of the afterglow). Similarly, as the O_2 gas flow was increased from 8 to 80 sccm, no significant change in ER or surface quality was observed.

B. Silicon etching

Figure 5 shows the silicon ER with respect to (a) incident ion energy and (b) percentage of SF_6 (by flow) in the $Ar-SF_6$ and O_2-SF_6 mixtures. In Fig. 5(a), the $Ar-SF_6$ plasma etches were operated for 2–4 min of processing time as the ion energy varied. Constant ERs of 130 nm/min at low (0–50 eV) energies and 1375 nm/min at high energies

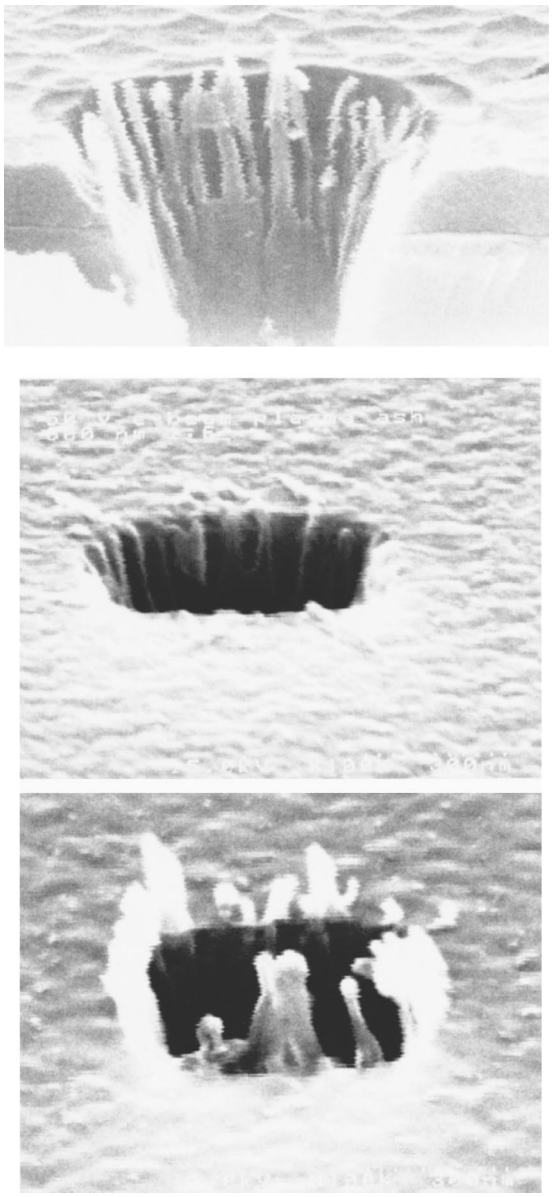

FIG. 3. Via structures etched in 55 mTorr O_2 plasma: (top) as received; (middle) after 50 eV etch; and (bottom) after 100 eV etch.

(150–250 eV) were seen, with a sharp transition occurring between 75 and 150 eV. For the 100 and 175 eV etches, SEM images of the SiO_2 masked samples are shown in Fig. 6. There was significant undercutting on the sample etched at 100 eV, whereas the sample etched at 175 eV showed a tapered feature with no visible undercutting. The lateral etch rate from the observed undercut in Fig. 6(a) was ≈200 nm/min. To determine the ER as the SF_6 flow was varied in the Ar–SF_6 mixtures [Fig. 5(b)], the ion energy (100 eV), operating pressure (65 mTorr), total flow (50 sccm), and processing time (3 min) were held constant. The ER increased with the SF_6 flow to a maximum value of 830 nm/min at ≈30%, then declined as the SF_6 flow increased further. None of these mixtures demonstrated a clear increase or decrease in the degree of undercutting except for the lowest SF_6 flow, which showed no significant undercutting but a reduced ER (500 nm/min). The reduction in the ER at the maximum SF_6 percentage also coincided with a reduction of the SF_6 partial pressure, presumably due to the

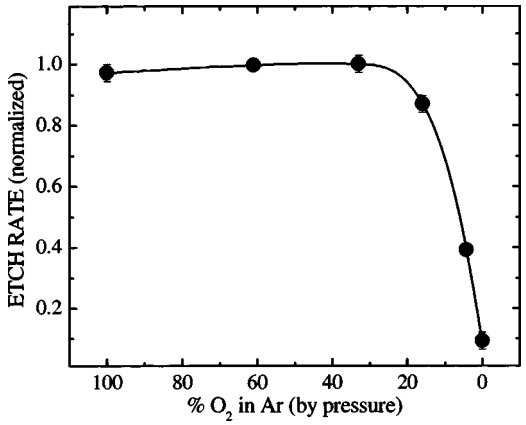

FIG. 4. Etch rate dependence of negative resist on O_2 percentage in gas feedstock mixture. Ion energy was held constant at 50 eV.

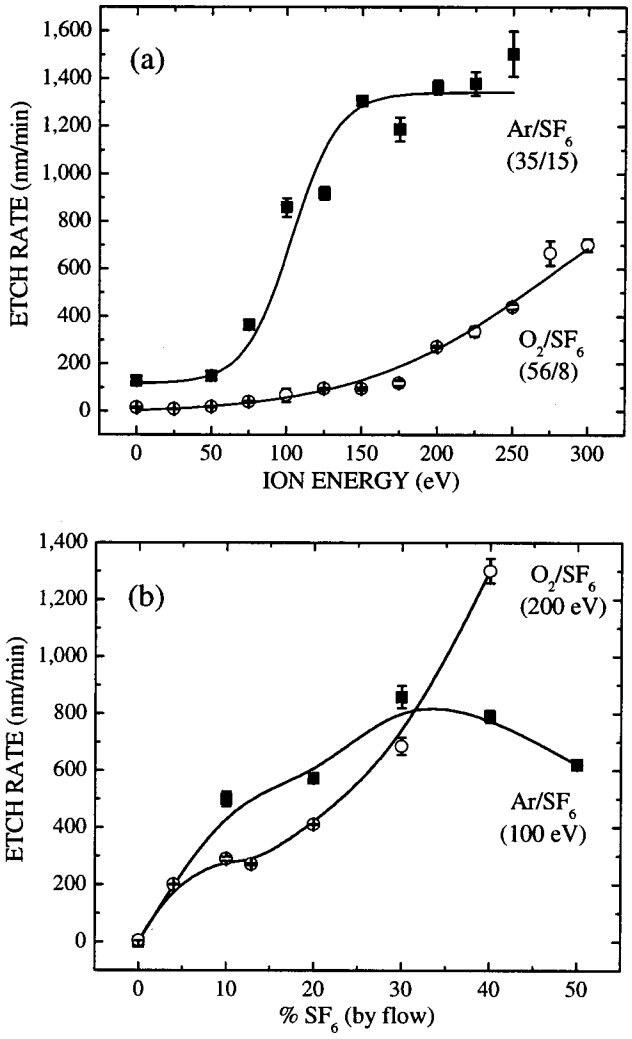

FIG. 5. Silicon etch rate dependencies with respect to (a) incident ion energy and (b) percentage of SF_6 flow in gas mixtures. Constant flows or energies are given on respective plots.

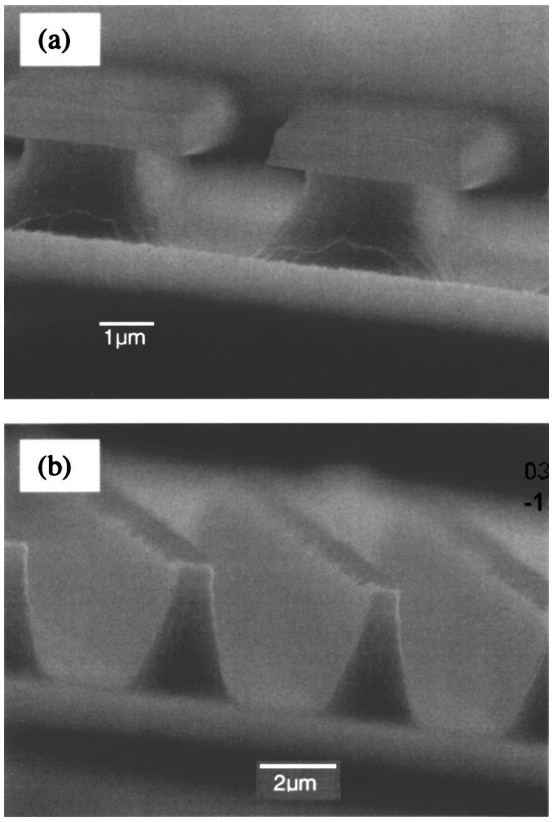

FIG. 6. SEM photographs of patterned silicon samples after $Ar-SF_6$ etch with (a) 100 eV and (b) 175 eV ion energies.

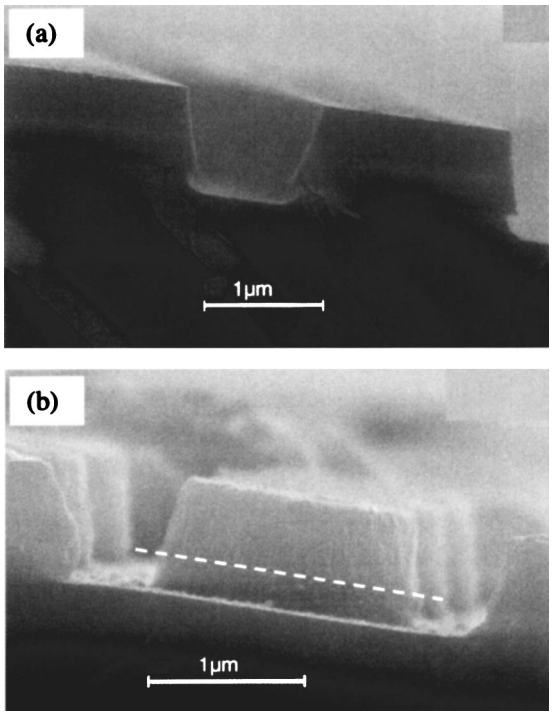

FIG. 7. SEM photographs of patterned silicon samples after O_2-SF_6 etch with (a) 50 eV and (b) 200 eV ion energies (dotted line shows mask–substrate interface).

varying pumping speed of the constituent gases. Although not actively measured in these experiments, it was likely that the e beam generation was reduced with the observed cathode current reduction, as the SF_6 concentration increased.

The O_2-SF_6 mixture ratio was 56:8 by flow and was operated at a total pressure of 60 mTorr for the ion energy dependence shown in Fig. 5(a), with 2–12 min process times. No etch selectivity between the SiO_2 mask and silicon substrate was observed in any of the O_2-SF_6 etching experiments; therefore, the higher energy processes were generally carried out for shorter exposure times. The ER was much lower than in the $Ar-SF_6$ mixtures and increased slowly from 15 to 120 nm/min as the ion energy was raised from 0 to 175 eV, then rose more sharply at higher energies. As in the argon mixture case, the process anisotropy increased with the ion energy, as shown by the SEM photographs in Fig. 7 for the 50 and 200 eV cases. Undercutting was seen beneath the mask in the lower energy case (50 eV), while the higher energy etch (200 eV) showed no undercutting. From the photos, the lateral etch rate was roughly 6.9 nm/min, which was much less than any ion-assisted etch rate shown in Fig. 5. As in the $Ar-SF_6$ mixtures, the ER increased rapidly with the percentage of SF_6 as shown in Fig. 5(b); however, black deposits formed on the substrates when the oxygen mixtures contained over 20% SF_6. As mentioned above, higher concentrations of SF_6 also appeared to degrade the e beam production in the hollow cathode.

Further investigations to optimize the etch processes were carried out by varying pulse lengths (0.5–10 ms) and duty cycle (1%–50%) for both the $Ar-SF_6$ and O_2-SF_6 mixtures, but no significant improvements were observed. No investigations of system micro-loading or feature-size dependent etching were carried out.

IV. DISCUSSION

A. Photoresist etching

From the data shown in Figs. 2 and 4 etching of the negative resist material in these experiments was an ion-driven process, given the direct correlation between ion energy and material removal. This dependence is not typically seen in plasma cleaning processes, which operate above the polymers' glass transition temperature (T_g) and focus on the flux of atomic oxygen to the surface for material removal. However, in a conventional plasma source the plasma potential may be 10–50 V and so even with a grounded stage, the energy of ions impinging on the surface will similarly be 10–50 eV in such a system. In contrast, plasma potentials in LAPPS are 1–5 V in molecular gases, so incident ion energies are low. In Fig. 2, resist removal was not automatic (exothermic) in the presence of the atomic oxygen generated in this system since the ER drops to nearly zero with no external bias. Thus, without any additional activation (i.e., ion energy, temperature), the formation and desorption of volatile etch species was not capable of progressing with measurable rates. These surface reactions are further hindered by the chemical structure of the negative resist, which

is a very stable unsaturated cyclic olefin. The dry processing of resist materials generally relies on desorption of carbon monoxide (CO) from the surface. Because the chemical composition of polymers varies, different mechanisms initiate the removal of material. The main removal mechanism appears to be random scission of the polymer chain, which proceeds through saturated (singly bonded) carbon atoms and is proportional to the flux of oxygen atoms.[15] Therefore, unsaturated carbon atoms must first become saturated before the attack of atomic oxygen is effective in breaking the polymer backbone. Similarly, polymers with aromatic groups are more etch resistant than nonaromatic polymers. (Furthermore, polymers containing carbonyl groups such as C═O or C–O more easily form CO under ion bombardment and in an oxygen deficient environment, have higher sputtering yields than compounds containing fully saturated structures.) Thus, in these experiments where the plasma potential was low and the substrate temperature was below the glass transition, it was not surprising that additional ion energy was needed to remove material. Therefore, the small sheath drop potential of the plasma allowed access to a broader processing range in this plasma system than is typically observed in etching organic materials. No material was removed without externally increasing the ion energy, however, when the ion energies ($<$100 eV) were moderately increased the resist material was rapidly removed. Furthermore, Fig. 4 shows that the plasma source was not limited in neutral flux, since the etch rate remained constant as the feedstock source of atomic oxygen (O_2) was reduced. Not until the molecular gas percentage dropped below 30% did the etch rate begin to fall. Above that concentration, it would be reasonable to assume that the dominant reactive species was atomic oxygen and argon ions impacting the surface promoted etching as well as oxygen ions. Additional support of the ion-driven resist removal in these experiments comes from the fact that the ER was independent of duty factor. The removal of material showed no dependence on the plasma afterglow between pulses, when neutral chemistry dominates as species continue to diffuse to the surface.

The results of the via residue removal in Fig. 3 show the importance of ions over a chemically driven (above T_g) process. The residues left behind from the cleaning process were easily removed with the assistance of 50 eV ions. With only a very fine (50 nm) residue in small feature sizes, any isotropic process would quickly destroy the original feature profile. Instead, after a clean removal of the residuals the via structure was left in tact. The residue formed at the higher ion energy (100 eV) was likely graphitization of the resist, which has been observed by others[4] and formed on this sample at the delicate spire-like structures. This experiment demonstrated the degree to which the ion energies can be controlled with electron beam generated plasmas and the subsequent reduction of graphitization in organic substrates.

B. Silicon etching

The formation of volatile silicon etch products, etch stop (capping) and passivating layers in SF_6-based plasmas has been discussed extensively in the scientific literature. In this section we discuss the issues of plasma formation and chemistry for an e beam generated plasma source used in place of a conventional discharge. Generally in these experiments, the etch rate was significantly larger for the $Ar-SF_6$ mixtures (up to 1500 nm/min at 250 eV) than for the O_2-SF_6 mixtures (up to 700 nm/min at 300 eV). While the plasma densities may have been larger in the $Ar-SF_6$ mixtures, the formation of a capping oxide layer likely caused the observed difference in etch rates.

Since silicon does not spontaneously etch in SF_6, etching was mainly driven by plasma-produced F radicals or F_2 (from recombination on the surface). Since all ionization and electronic excitation channels of SF_6 are dissociative and dissociative attachment[16] in SF_6 is large for low energy electrons, an abundance of atomic fluorine is expected in conventional discharges as well as these plasmas. The etching results from these $Ar-SF_6$ mixtures can be understood as follows: The primary etchant, atomic fluorine, was readily produced (as in other systems), which resulted in a chemical ER of $\sim$200 nm/min laterally (undercut) and 130 nm/min vertically from the data shown in Figs. 6(a) (100 eV) and 5(a) (0 eV case), respectively. (These rates cannot be *directly* compared, as the effects of ion energy cannot be completely decoupled.) At higher ion energies, the ion-driven (vertical) ER greatly exceeded the chemical (lateral) ER, which allowed shorter exposure times and resulted in less undercutting. The pyramidal bases of the structures [Fig. 6(b)] are believed to be due to charging of the insulating SiO_2 mask, which would deflect ion trajectories as they passed the structures, resulting in the observed features. (Neither lateral or vertical mask erosion was observed in these experiments.) Finally, the increase in the ER with the SF_6 flow and the roll-off above 30% SF_6 [Fig. 5(b)] caused by a change in system pumping suggests the ER varies directly with the SF_6 partial pressure. The system pumping change, while difficult to quantify without mass spectrometry measurements, was believed to cause a disparate pumping of the constituent gases and result in a decrease in the SF_6 partial pressure. This trend is reasonable, since the SF_6 pressure directly affects the concentration of the primary etchant (F).

The ERs reported here are comparable to recent values achieved in other nonoptimized high-density plasma reactors by Herrick *et al.*[3] although are 2 to 3 times lower than well-developed time-multiplexed[8] techniques. Herrick similarly observed that the ER depended strongly on atomic fluorine concentration but was independent of the ion energy and that etching continued into the afterglow of a pure SF_6 plasma. These differences may be due to the low-pressure (mTorr) helicon source being used and its inherently higher plasma potential, which could transport hot ("hyperthermal") F atoms to the silicon surface and supply sufficient ion energy to rapidly desorb volatile species.

While fluorine is the obvious etchant in this system, plasma ion species are critical as well. The primary ion species produced by a 2 keV electron beam[17] in SF_6 are SF_5^+ followed by SF_3^+. The massive SF_5^+ ion can also be pro-

duced by charge exchange with Ar^+, which is quite rapid[18] ($k_{ce} \sim 10^{-9}$ cm^3/s). Hence in these plasmas, the flux of SF_5^+ dominates Ar^+ for all but the smallest concentrations of SF_6.[19] Therefore, even a small amount of SF_6 in these gas mixtures produce a plasma rich in reactive ion *and* radical species, as illustrated by the rapid rise of ER with SF_6 flow shown in Fig. 5(b). Furthermore, heavier (and possibly more reactive) ions can impact the surface to stimulate desorption and ion-assisted etching. This is in contrast to previous findings in conventional inductive[20] and capacitively[21] coupled discharges, where SF_3^+ and S^+ are the dominant ions, respectively. In conventional discharges the plasma electrons preferentially dissociate SF_6, leading to the ionization of the molecular fragments, which are known[22] to have lower ionization potentials than the parent molecule. This results in a lower average ion mass impinging on the surface.

The lower ER of silicon in the O_2-SF_6 mixtures compared to the $Ar-SF_6$ mixtures is believed to be due to the redeposition or growth of $SiO_x(F_y)$ complexes[23] on the surface. For the O_2-SF_6 data shown in Fig. 5(a), the plasmas (and ion densities) were identical, and therefore the observed changes with incident ion energy were due to the competition between deposition and evolution of volatile etch products. Since the formation of oxides and oxyfluorides on exposed silicon quench chemical etching and are considered the key to anisotropic pattern transfer for such chemistries, these results are not entirely unexpected. Hasan *et al.*[24] added O_2 to SF_6 plasmas to etch poly-silicon and found that the addition of O_2 significantly raised the temperature at which anisotropic etching can be obtained. In those experiments, gas mixtures of less than 50% oxygen demonstrated highly anisotropic etching at $-100\,^\circ$C, with a decrease in sidewall angle to 60° at room temperature, for 10 eV ions. The etch rates were consistently 110 nm/min for all temperatures. In the present experiments, higher O_2 gas ratios were necessary for the e beam production (i.e., cathode operation), which likely resulted in larger fluxes of oxygen radicals and ions interacting with the silicon surface. The O^+ ion flux is dominant[11] in e beam produced oxygen plasmas but are somewhat reduced in these mixtures by dissociative charge transfer ($O^+ + SF_6 \rightarrow SF_5^+ + FO$) to make a more massive reactive ion. (The O_2^+ ion is not reactive with SF_6 so it primarily recombines in the gas phase or at the surface.) These relationships imply that the formation of the $SiO_x(F_y)$ capping layer (and consequently low etch rates) in the O_2-SF_6 experiments was due to the flux of oxygen radicals. A large flux of oxygen radicals in these mixtures could oxidize the silicon surface before the silicon fluoride etch products were able to form, causing the process to be more like silicon oxide etching and thereby reduce the selectivity over the SiO_2 mask, as was observed. Auger or x-ray photoelectron spectroscopies (XPS) could be used to substantiate these findings, but are presently unavailable. The discoloration of the sample surface with increasing SF_6 flow was likely due to increased SiO_xF_y formation over SiO_x and consequently excessive micromasking. These micromasks along with an increased ER [Fig. 5(b)] and profile anisotropy allow the surface features to trap and scatter light, which visually gives the appearance of roughened grey–black surfaces ("black silicon"[25]). The SEM photographs in Fig. 7 show the surfaces to be both well-passivated and rougher, compared to Fig. 6(a). The photographs also indicate a greatly reduced (lateral) chemical etch component ($\approx$7 nm/min). Unfortunately, since the electron beam production was unstable with the increase in SF_6 flow, only limited experiments could be performed.

V. SUMMARY

A $25 \times 50 \times 1$ cm^3 electron-beam produced plasma sheet was used to remove photoresist material and $\langle 100 \rangle$ silicon. The 2 keV electron beam was produced by a modulated hollow cathode source in a uniform 165 Gauss magnetic field. Gas compositions primarily consisted of oxygen at 55 mTorr for the resist removal, while mixtures of argon or oxygen with sulfur hexafluoride at $\sim$60 to 70 mTorr were used for the silicon etching. These plasmas characteristically have electron temperatures $\sim$0.5 eV, plasma potentials $<$3 V and electron densities of $1-5 \times 10^{11}$ cm^{-3} in the bulk of the plasma.

Significant dependencies of the etch rate on ion energies (controlled by an external rf bias) and gas compositions were observed. Specifically for the resist material, etch rates increased nearly linearly from 50 to 225 nm/min as ion energies were increased from 25 to 100 eV. Anisotropy of patterned features also increased with ion energy, with good pattern transfer above 50 eV. As the oxygen percentage in the feedstock gas decreased, the etch rate remained constant until the oxygen concentration fell below 30%, implying that the flux of neutral atomic species was abundant in this plasma source.

A large disparity in the silicon etch rate was observed for the $Ar-SF_6$ and O_2-SF_6 mixtures, with etch rates five times greater in the Ar mixtures. At maximum ion energies of 300 eV, the O_2-SF_6 mixture reached an etch rate of 700 nm/min, while the $Ar-SF_6$ mixture had an etch rate of 1375 nm/min at 200 eV. There was strong competition between deposition and etching processes in the O_2 mixtures, which led to the different etch rates. The data suggested that the oxygen mixtures readily formed an involatile $SiO_x(F_y)$ capping layer, which eventually sputtered away as the ion energy was increased. Increasing the relative SF_6 flows in these mixtures correspondingly increased the process etch rate due to increased atomic F concentration, until the system gas pumping changed ($Ar-SF_6$ mixtures) or the oxyfluoride film micromasked the exposed surfaces.

VI. CONCLUSION

In this work, e beam generated oxygen plasmas were shown to offer a high degree of control in removing photoresist material anisotropically. The rate of removal varied strongly with ion energy, which indicates that ions were able to contribute significantly to this process (likely through the stimulated desorption of etch products). Additionally, experiments showed that e beam generated plasmas provide an

abundance of free radical oxygen atoms, which allowed less oxygen to be used in the process gas mixture. The additional process control demonstrated shows great promise in delicate material modification, including surface activation as well as bulk removal of material for e beam generated plasmas. Further investigations using other polymer substrates and activation energies (including above the glass transition temperature) would complement these initial findings and offer a complete set of process control variables. However, the appreciable room temperature etch rates, high degree of process control and scaling possibilities of the plasma source make it a viable etching system for delicate materials' processes.

In SF_6-based systems, initial experiments with these plasma sources have etched silicon at room temperature without significant undercutting of large (2 to 3 micron) features, with rates exceeding 1 μm/min. Ion chemistries favor more massive molecular ions, specifically SF_5^+ as opposed to conventional discharges, which tend to dissociate large molecules and create lower molecular weight ions. The differences in plasma chemistry between O_2-SF_6 and $Ar-SF_6$ in this system are believed to be caused by atomic oxygen radicals forming a tough $SiO_x(F_y)$ capping layer. The effects of passivating films on the etching process can be improved greatly in this system using tertiary gas mixtures such as $Ar-O_2-SF_6$ or O_2-SF_6-fluorocarbon mixtures; either would allow less oxide formation without sacrificing electron beam operation. Jansen *et al.*[25] investigated feature evolution with similar passivating layers on room temperature substrates. In that work, CHF_3 was added to the O_2-SF_6 gas mixture to eliminate the thin passivating oxyfluoride film from the trench bottoms. At high oxygen concentrations, these films would produce micromasked features ("grass") if not undercut by the additional CF_x species. Once the deposition of the passivating films is better controlled, the dependence of the plasma duty factor could be used to enhance feature evolution.

A separable electron beam source would also improve overall system performance, because the process gas mixtures could then be varied while keeping the e beam properties fixed. This was a major obstacle in the O_2-SF_6 experiments. With a constant e beam source, much higher etch rates and larger ranges of process chemistry would be available for silicon etching in this system. Although a complete explanation of all observations is presently not possible, the purpose of this work was to present initial findings and identify the underlying plasma chemistry and physics involved with e beam generated plasmas. The use of these e beam generated plasmas for etching applications has been shown to be quite plausible and offered additional control over process parameters (ion energy and some ion chemistry) not observed in other plasma processing systems. This additional control is primarily due to the low electron temperatures of the bulk plasma and the unique ionization mechanism used to create the plasma.

ACKNOWLEDGMENTS

A significant portion of this work could not have been completed without the technical support of Mr. Tony Noll (NRL) and Robert Lanham (SFA Inc.) and undergraduate student Amy Perlman (SFA Inc.). The helpful conversations and assistance of Dr. John Hallock and Axcelis Technologies (Rockville, MD) were greatly appreciated, as well as the via samples and their *ex situ* analyses. The Office of Naval Research supported this research.

[1] D. L. Flamm, in *Plasma Etching: An Introduction*, edited by D. M. Manos and D. L. Flamm (Academic, New York, 1989), p. 131.
[2] K.-M. Chang, T.-H. Yeh, I.-C. Deng, and H.-C. Lin, J. Appl. Phys. **80**, 3048 (1996).
[3] A. Herrick, A. J. Perry, and R. W. Boswell, J. Vac. Sci. Technol. A **21**, 955 (2003).
[4] S. W. Pang, K. T. Sung, and K. K. Ko, J. Vac. Sci. Technol. B **10**, 1118 (1992).
[5] O. Joubert, J. Pelletier, and Y. Arnal, J. Appl. Phys. **65**, 5096 (1989).
[6] M. Zeuner, J. Meichsner, and H.-U. Poll, Plasma Sources Sci. Technol. **4**, 406 (1995).
[7] E. J. H. Collart, J. A. G. Baggerman, and R. J. Visser, J. Appl. Phys. **78**, 47 (1995).
[8] A. A. Ayón, R. Braff, C. C. Lin, H. H. Sawin, and M. A. Schmidt, J. Electron. Mater. **146**, 339 (1999).
[9] R. F. Fernsler, W. M. Manheimer, R. A. Meger, J. Matthew, D. P. Murphy, R. E. Pechacek, and J. A. Gregor, Phys. Plasmas **5**, 2137 (1998).
[10] W. M. Manheimer, R. F. Fernsler, M. Lampe, and R. A. Meger, Plasma Sources Sci. Technol. **9**, 370 (2000).
[11] D. Leonhardt, S. G. Walton, D. D. Blackwell, D. P. Murphy, R. F. Fernsler, and R. A. Meger, J. Vac. Sci. Technol. A **19**, 1367 (2001).
[12] S. G. Walton, D. Leonhardt, D. D. Blackwell, D. P. Murphy, R. F. Fernsler, and R. A. Meger, J. Vac. Sci. Technol. A **19**, 1325 (2001).
[13] M. C. Myers, D. D. Hinshelwood, R. A. Meger, and R. E. Pechacek, Proceedings of the 12th IEEE Pulse Power Conference, Monterey, CA (1999). This unit was designed to provide currents in excess of 1 A/pulse.
[14] M. F. Doemling, N. R. Rueger, G. S. Oehrlein, and J. M. Cook, J. Vac. Sci. Technol. A **16**, 1998 (1998).
[15] S. R. Cain, F. D. Egitto, and F. Emmi, J. Vac. Sci. Technol. A **5**, 1578 (1987).
[16] R. d'Agostino and D. L. Flamm, J. Appl. Phys. **52**, 162 (1981).
[17] R. Rejoub, D. R. Sieglaff, B. G. Lindsay, and R. F. Stebbings, J. Phys. B **34**, 1289 (2001).
[18] F. C. Fehsenfeld, J. Chem. Phys. **54**, 438 (1971).
[19] S. G. Walton, D. Leonhardt, R. F. Fernsler, and R. A. Meger, Appl. Phys. Lett. **81**, 987 (2002); S.G.W. provided the results for various SF_6 concentrations were given as a private communication.
[20] A. N. Goyete, Y. Wang, and J. K. Olthoff, J. Vac. Sci. Technol. A **19**, 1294 (2001).
[21] R. Forest, J. K. Olthoff, R. J. Van Brunt, E. C. Benck, and J. R. Roberts, Phys. Rev. E **54**, 1876 (1996).
[22] M. A. Ali, K. K. Irikura, and Y.-K. Kim, Int. J. Mass. Spectrom. **21**, 187 (2000).
[23] Since there was no definitive identification of the passivation layer, the formula $SiO_x(F_y)$ is used to represent either SiO_x of SiO_xF_y compounds.
[24] I. Hasan, C. A. Pawlowicz, L. P. Benet, and N. G. Tarr, J. Vac. Sci. Technol. A **20**, 983 (2002).
[25] H. Jansen, M. de Boer, R. Legtenberg, and M. Elwenspoek, J. Micromech. Microeng. **5**, 115 (1995).